

Physical and Electrical Performance of Vapor–Solid Grown ZnO Straight Nanowires

J. Y. Li · H. Li

Received: 14 October 2008 / Accepted: 11 November 2008 / Published online: 3 December 2008
© to the authors 2008

Abstract Physical and electrical properties of wurtzitic ZnO straight nanowires grown via a vapor–solid mechanism were investigated. Raman spectrum shows four first-order phonon frequencies and a second-order Raman frequency of the ZnO nanowires. Electrical and photoconductive performance of individual ZnO straight nanowire devices was studied. The results indicate that the nanowires reported here are n-type semi-conductors and UV light sensitive, and a desirable candidate for fabricating UV light nanosensors and other applications.

Keywords Nanostructures · Nanosensors · ZnO

Introduction

Wurtzite structure zinc oxide (ZnO) is a very important II–VI group semiconductor. It has a direct wide bandgap of 3.37 eV, higher exciton binding energy (60 meV for ZnO vs. 28 meV for GaN), and higher optical gain (300 cm^{-1} for ZnO versus 100 cm^{-1} for GaN) at room temperature [1–4]. Recently, ZnO has attracted extensive interest for its applications in numerous fields. It is of interest for low-voltage and short wavelength (green or green/blue) electro-optical devices such as light emitting diodes and laser diodes. It also can be widely used as transparent ultraviolet (UV)-protection films, transparent conducting oxide

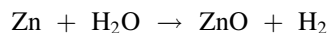
materials, piezoelectric materials, electron-transport medium for solar cells, chemical sensors, photo-catalysts, and so on [1–4].

In the past few years, extensive reports regarding the study of ZnO nanowires continue at a dizzying pace for their great prospects in fundamental physical science, novel nano-technological applications, and significant potential for nano-optoelectronics, and nano-ZnO was suggested to be the next most important nano-material after carbon nanotubes [5–14].

Herein, we report the physical and electrical properties of vapor–solid grown ZnO straight nanowires. The ZnO straight nanowires were grown via a facile catalyst-free method on amorphous fused quartz surfaces on a large-scale. Raman spectra of the ZnO nanowires were investigated. Individual ZnO straight nanowire devices were fabricated, and photoconductive and electrical studies were carried out with the single ZnO nanowire devices.

Experimental

The system used to grown ZnO straight nanowires is similar to that in our previous report [15], and the ZnO nanowires were grown in a horizontal fused quartz tube inside a conventional tube furnace. The reaction through which the ZnO nanowires synthesized can be expressed as:



As a precursor, high pure metal zinc powders were loaded into the center of the tube. The vapor H_2O was carried into the quartz tube through the flow of high pure argon. At high temperature (700–800 °C) zinc reacted with vapor H_2O and produced ZnO nanowires. The nanowires were deposited on amorphous fused quartz substrates.

J. Y. Li (✉)

Department of Physical Chemistry, University of Science and Technology Beijing, Beijing, China
e-mail: physchemustb@gmail.com

H. Li

Institute of Microstructure and Properties of Advanced Material, Beijing University of Technology, Beijing, China

Results and Discussion

X-ray diffraction (XRD) examination was used to assess the overall crystallographic properties and phase purity of the product. Figure 1 shows a powder XRD pattern of the as-grown ZnO nanowires and it reveals that the nanowires are composed of hexagonal ZnO. The positions of the XRD peaks show good agreement with those of the reported standard data of hexagonal ZnO with lattice constants $a = 0.3250$ nm and $c = 0.5207$ nm (Joint Committee on Powder Diffraction Standards (JCPDS) Card No. 36–1451). The strong intensities of the ZnO diffraction peaks relative to the background signal indicate that the as-grown nanowires are high pure hexagonal phase ZnO. The structure of the ZnO nanowires was further characterized by selected area electron diffraction (SAED). Inset of Fig. 1 (right) is an SAED pattern of an individual ZnO nanowire. The SAED pattern can be indexed as a hexagonal structure with lattice constants of $a = 0.325$ nm and $c = 0.52$ nm, which is in good agreement with the XRD result. The SAED pattern reveals the single-crystalline hexagonal phase nature of the ZnO nanowires. Inset of Fig. 1 (left) is a typical field emission scanning electron microscope (FESEM) image of the ZnO nanowires, and it shows the nanowires with diameters of several tens nanometers. Most of the nanowires have length of several to tens microns. The nanowires are straight and most of them show smooth surface and no ramification over their length.

The vapor–liquid–solid (VLS) mechanism is common for the catalyzed growth of one-dimensional materials, and catalyst particles are typically detected at tips of the VLS grown one-dimensional materials [16]. In the present case,

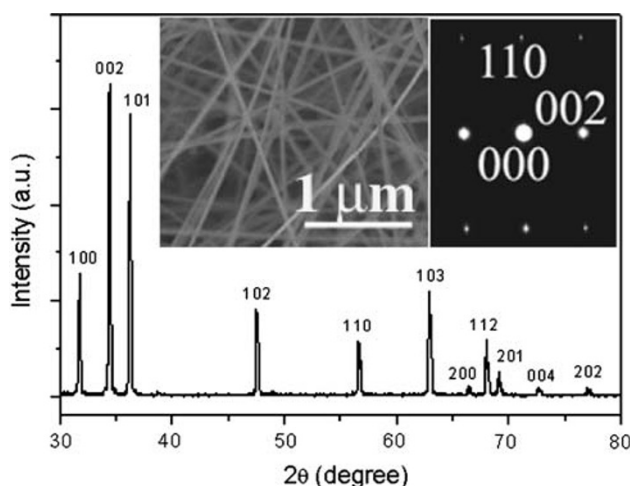


Fig. 1 Room temperature powder XRD pattern of the ZnO straight nanowires using Cu K α radiation and the (hkl) values of the hexagonal ZnO are specified about the diffraction peaks. Inset (left) is a typical FESEM image of the nanowires, and inset (right) is a SAED pattern of the ZnO nanowire

however, the VLS mechanism is not responsible for explaining the growth of the ZnO nanowires. This is because there is no catalyst used in the growing process, and no catalyst particles are detected at the ZnO nanowire tips. It appears the growth of the ZnO straight nanowires reported here occurs via a vapor–solid (VS) mechanism [17]. The vapor H₂O was carried into the quartz tube and transported downstream by the flow of argon. At the center of the tube furnace, metal zinc vaporized and reacted with vapor H₂O to generate ZnO vapor. Then the ZnO vapor deposited on the substrates and nucleation of wurtzite structure ZnO nanoparticles (nanorods) took place. Through a VS growth mechanism, the ZnO nanoparticles (nanorods) prolonged and the solid ZnO long nanowires were formed.

Raman scattering spectrum is a very useful tool for the structure characterization of nanomaterials. Wurtzite structure ZnO possesses four atoms per primitive cell and the space group of wurtzite structure is $C_{6v}^4 (P6_3mc)$ with all atoms occupying the C_{3v} sites. According to the factor group analysis, single crystal wurtzite structure ZnO possesses eight sets of optical phonon modes near the zone center. The modes are classified into Raman allowed ($A_1 + E_1 + 2E_2$), infrared allowed ($A_1 + E_1$), and both Raman and infrared silent ($2B_1$). The A_1 and E_1 modes, corresponding to optical phonons, will split into a longitudinal-optical (LO) and a transverse-optical (TO) component due to the macroscopic electrical field associated with the longitudinal vibration [18–20]. The high frequency E_2 mode involves only the oxygen atoms, and the low frequency E_2 mode is associated with the vibration of the heavy Zn sub-lattice [21].

Figure 2 is a Raman scattering spectrum of the ZnO straight nanowires in the frequency range from 250 to 750 cm^{-1} . Four first-order Raman-active phonon bands of wurtzite structure ZnO are observed. The most intense peak at 440 cm^{-1} corresponds to non-polar optical phonon E_2 (high) of wurtzitic ZnO, and it is a particularly important feature characteristic of hexagonal phase ZnO. The bands 380 cm^{-1} and 410 cm^{-1} agree with phonon vibration frequencies of A_1 (TO) and E_1 (TO) modes of wurtzite ZnO, respectively. The peak at 586 cm^{-1} is attributed to the E_1 (LO) mode of hexagonal ZnO, and it is associated with oxygen deficiency. The Raman peak at 334 cm^{-1} is assigned to the second-order Raman spectrum arising from zone-boundary phonons of hexagonal ZnO, and the data agree well with previous reports on wurtzite structure ZnO crystal samples [20] and thin films [21].

It can be also found from Fig. 2 that the Raman spectrum of the ZnO nanowires is slightly asymmetrical with respect to those of ZnO crystals [20]. This asymmetrical spectrum shape is mainly attributed to the confinement effects of phonons in nanowire samples. The phonons can

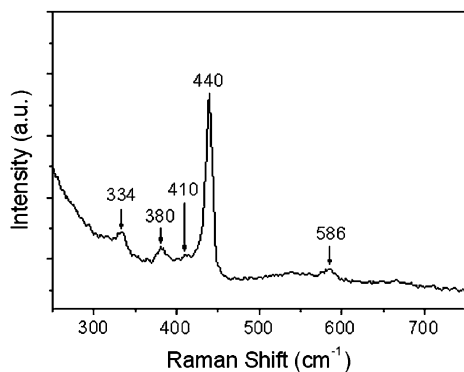


Fig. 2 Raman-scattering spectrum of the ZnO straight nanowires measured with a 488 nm excitation at room temperature

be confined within the nanosized systems and thus phonons other than those of Brillouin-zone center can also contribute to the Raman spectrum, which leads to the asymmetrical shapes of the Raman spectrum. Such an asymmetrical shape of the Raman modes associated with the phonon confinement effects in ZnO nano-sized systems are also reported on ZnO nanoparticles [22].

To test photoconduction of the individual ZnO straight nanowires, single ZnO nanowire field effect transistors were fabricated by e-beam lithographic technique [23], and the photoconductive studies were carried out with the single ZnO nanowire devices. The electrical measurements were performed at room temperature. Figure 3a shows the room temperature current versus voltage plots of a single ZnO nanowire device measured with and without 254 nm short wave UV light illumination. The linear I–V behavior indicates the ohmic contacts between the electrodes and the ZnO nanowire. As is expected for semiconducting ZnO nanowires, under UV illumination, the conductivity of the nanowire greatly increases due to the photo-generated carriers in the semiconducting ZnO nanowire. UV light (254 nm) has photon energy of 4.88 eV, large enough to excite electrons across the bandgap of ZnO (3.37 eV). The photoconduction result indicates the ZnO straight nanowires reported here are UV light sensitive and a desirable candidate for nano-scale UV light sensors. Figure 3b is a set of typical room temperature I_{sd} vs. V_{sd} data of the individual ZnO nanowire device recorded at different gate voltages. The conductance of the ZnO nanowire decreases with increasingly negative gate voltages. From the gate-dependence of the I_{sd} vs. V_{sd} curves, the ZnO nanowire can be identified as a very fine n-type semiconductor. In other words, the transport through the ZnO nanowires is dominated by negative carriers. The results reveal that the straight ZnO nanowires reported here can serve as building blocks for the assembly of nanodevices for applications in nanoscale science and technology. The ZnO Nanowires grown from this facile method is large-scale growth, cheap

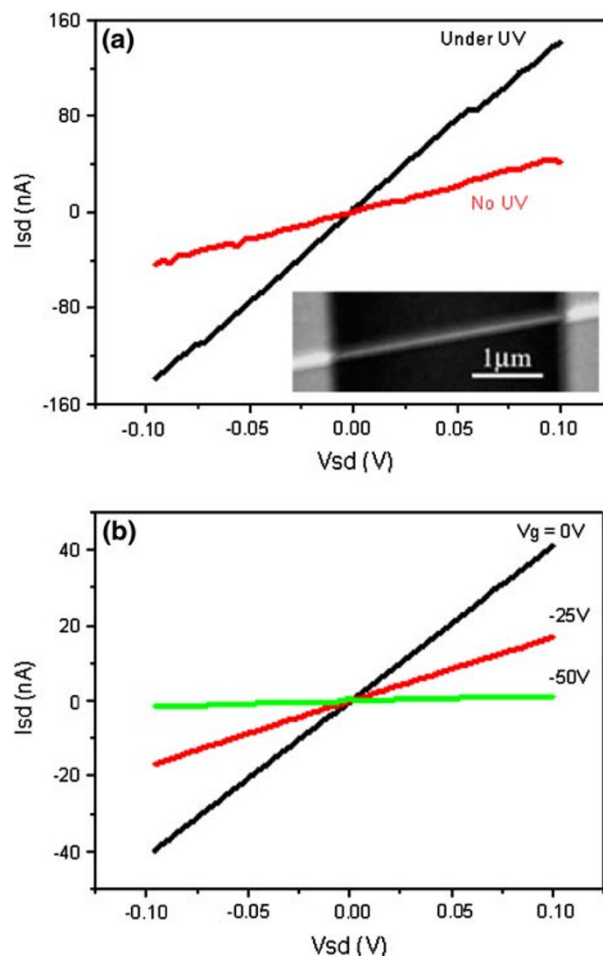


Fig. 3 **a** Room temperature current versus voltage plots of an individual ZnO straight nanowire device measured with and without 254 nm UV light illumination; inset: SEM image of the individual ZnO nanowire device. **b** Room temperature gate-dependent I_{sd} vs V_{sd} curves of the individual ZnO nanowire device

(only use amorphous fused quartz substrates), and pure (no contamination from catalyst), this facile technique will greatly facilitate the large-scale industrial production and applications of ZnO Nanowires.

Conclusions

In conclusion, the physical and electrical properties of vapor–solid grown hexagonal ZnO straight nanowires were investigated. The Raman spectrum shows four first-order phonon frequencies of E_2 (high) = 440 cm^{-1} , A_1 (TO) = 380 cm^{-1} , E_1 (TO) = 410 cm^{-1} , and E_1 (LO) = 586 cm^{-1} ; and a second-order Raman spectrum at 334 cm^{-1} which arises from zone-boundary phonons of hexagonal ZnO. Individual ZnO straight nanowire devices were fabricated and the electrical and photoconductive studies were carried out with the single nanowire devices. The result

indicates that the ZnO straight nanowire is a fine n-type semiconductor and a desirable candidate for fabricating UV light nano-sensors and other applications.

References

1. E.M. Wong, P.C. Searson, *Appl. Phys. Lett.* **74**, 2939 (1999). doi: [10.1063/1.123972](https://doi.org/10.1063/1.123972)
2. E.A. Meulenkaamp, *J. Phys. Chem. B* **102**, 5566 (1998). doi: [10.1021/jp980730h](https://doi.org/10.1021/jp980730h)
3. S. Choopun, R.D. Vispute, W. Noch, A. Balsamo, R.P. Sharma, T. Venkatesan, A. Iliadis, D.C. Look, *Appl. Phys. Lett.* **75**, 3947 (1999). doi: [10.1063/1.125503](https://doi.org/10.1063/1.125503)
4. M.H. Huang, S. Mao, H. Feick, H.Q. Yan, Y. Wu, H. Kind, E. Weber, R. Russo, P.D. Yang, *Science* **292**, 1897 (2001). doi: [10.1126/science.1060367](https://doi.org/10.1126/science.1060367)
5. J.Y. Lao, J.G. Wen, Z.F. Zen, *Nano Lett.* **2**, 1287 (2002). doi: [10.1021/nl025753t](https://doi.org/10.1021/nl025753t)
6. M. Law, L.E. Greene, J.C. Johnson, R. Saykelly, P.D. Yang, *Nat. Mater.* **4**, 455 (2005). doi: [10.1038/nmat1387](https://doi.org/10.1038/nmat1387)
7. Z.L. Wang, J.H. Song, *Science* **312**, 242 (2006). doi: [10.1126/science.1124005](https://doi.org/10.1126/science.1124005)
8. J.V. Foreman, J.Y. Li, H.Y. Peng, S.J. Choi, H.O. Everitt, J. Liu, *Nano Lett.* **6**, 1126 (2006). doi: [10.1021/nl060204z](https://doi.org/10.1021/nl060204z)
9. B. Xiang, P.W. Wang, X.Z. Zhang, S.A. Dayeh, D.P.P. Aplin, C. Soci, D.P. Yu, D.L. Wang, *Nano Lett.* **7**, 323 (2007). doi: [10.1021/nl062410c](https://doi.org/10.1021/nl062410c)
10. X. Shen, P.B. Allen, J.T. Muckerman, J.W. Davenport, J.C. Zheng, *Nano Lett.* **7**, 2267 (2007). doi: [10.1021/nl070788k](https://doi.org/10.1021/nl070788k)
11. L. Shi, Y.M. Xu, S.K. Hark, Y. Liu, S. Wang, L. Peng, K. Wong, Q. Li, *Nano Lett.* **7**, 3559 (2007). doi: [10.1021/nl0707959](https://doi.org/10.1021/nl0707959)
12. Y.M. Oh, K.M. Lee, K.H. Park, Y. Kim, Y.H. Ahn, J. Park, S. Lee, *Nano Lett.* **7**, 3681 (2007). doi: [10.1021/nl071959o](https://doi.org/10.1021/nl071959o)
13. S. Ruhle, L.K. van Vugt, H.Y. Li, N.A. Keizer, L. Kuipers, D. Vanmaekelbergh, *Nano Lett.* **8**, 119 (2008). doi: [10.1021/nl0721867](https://doi.org/10.1021/nl0721867)
14. W.K. Hong, J.I. Sohn, D.K. Hwang, S. Kwon, G. Jo, S. Song, S. Kim, M.E. Welland, T. Lee, *Nano Lett.* **8**, 950 (2008). doi: [10.1021/nl0731116](https://doi.org/10.1021/nl0731116)
15. J.Y. Li, X.L. Chen, H. Li, M. He, Z.Y. Qiao, *J. Cryst. Growth* **233**, 5 (2001). doi: [10.1016/S0022-0248\(01\)01509-3](https://doi.org/10.1016/S0022-0248(01)01509-3)
16. A.M. Morales, C.M. Lieber, *Science* **279**, 208 (1998). doi: [10.1126/science.279.5348.208](https://doi.org/10.1126/science.279.5348.208)
17. J.Y. Li, H.Y. Peng, J. Liu, H.O. Everitt, *Eur. J. Inorg. Chem.* 3172 (2008). doi: [10.1002/ejic.200701306](https://doi.org/10.1002/ejic.200701306)
18. J.M. Calleja, M. Cardona, *Phys. Rev. B* **16**, 3753 (1977). doi: [10.1103/PhysRevB.16.3753](https://doi.org/10.1103/PhysRevB.16.3753)
19. M. Cardona, G. Guntherodt (eds.), *Topics in Applied Phys (Vol. 50)—Light Scattering in Solids II* (Springer-Verlag, Berlin, 1982)
20. T.C. Damen, S.P. Porto, B. Tell, *Phys. Rev.* **142**, 570 (1966). doi: [10.1103/PhysRev.142.570](https://doi.org/10.1103/PhysRev.142.570)
21. M. Koyano, P. Quocbao, L.T. Thanhbinh, L. Hongha, N. Ngoclong, S. Katayama, *Phys. Status Solidi (a)* **193**, 125 (2002). doi: [10.1002/1521-396X\(200209\)193:1<125::AID-PSSA125>3.0.CO;2-X](https://doi.org/10.1002/1521-396X(200209)193:1<125::AID-PSSA125>3.0.CO;2-X)
22. Y. Du, M.S. Zhang, J. Hong, Y. Shen, Q. Chen, Z. Yin, *Appl. Phys. A* **76**, 171 (2003). doi: [10.1007/s003390201404](https://doi.org/10.1007/s003390201404)
23. J.Y. Li, L. An, C.G. Lu, J. Liu, *Nano Lett.* **6**, 148 (2006). doi: [10.1021/nl051265k](https://doi.org/10.1021/nl051265k)